Predicting speciation in the multi-component equilibrium self-assembly of a metallosupramolecular complex

Thomas M. Fyles* and Christine C. Tong

Received (in Durham, UK) 21st September 2006, Accepted 29th November 2006
First published as an Advance Article on the web 16th January 2007
DOI: 10.1039/b613758j

A practical method to predict the speciation in a multi-component equilibrium self-assembly process has been developed and applied to the formation of the square macrocyclic complex formed from (ethylenediamine)Pd(II) and 4,4′-bipyridyl. The method is based on an additive free energy approach that derives the cumulative formation constants of all 56 species at equilibrium from a set of five pair-wise interactions. Estimates for the required values of the pair-wise interactions were derived from potentiometric titration of (ethylenediamine)Pd(II) and 3-phenylpyridine, and from (diethylenetriamine)Pd(II) and 4,4′-bipyridyl systems. The method calculates the equilibrium speciation as a function of reactant concentrations and pH and produces a map of the range of compositions in which the square complex and competing species are dominant. The predictions of the method closely correlate with available experimental data.

Introduction

Equilibrium self-assembly—the spontaneous formation of ordered supramolecular structures from molecular components *via* reversible intermolecular interactions[1–3]—is a core concept of modern supramolecular chemistry. Although most current reports emphasize the formation of complex and aesthetically pleasing structures,[2,3] the potential of self-assembly will only be realized in the functions of the species produced.[4–7] Supramolecular functions, such as encapsulation, molecular recognition, catalysis and transport arise *via* additional intermolecular interactions that compete with the self-assembly process. The discussion of the key thermodynamic features of self-assembly is most developed for metallosupramolecular complexes, particularly helicates,[8–11] and is principally directed to probing the nature of cooperativity in these assemblies. We approach the area from the perspective of the design of new functional self-assembled supramolecular assemblies in which an appreciation of the overall thermodynamics of these complex systems is an essential design component. Consequently, we seek ways to work within a sound thermodynamic framework to predict the formation of a self-assembled component that could play a functional role.

Although our goals are general, we focus here on a specific example of how this design process might proceed in the expectation that the approach will be amenable to application in other systems. Our example is based on the "square" palladium complex reported by Fujita *et al.*[12,13] (Scheme 1) This complex forms spontaneously in aqueous solution at room temperature from an equimolar mixture of (ethylenediamine)palladium(II) dinitrate (**enPd**$(NO_3)_2$) and 4,4-bipyridyl (**bipy**). The functional capability of this complex for molecular recognition of aromatic guests in water has been demonstrated.[13,14] Our interest is in the use of this complex as a macrocyclic portal to an ion channel. We envisage a suitably lipophilic derivative of either or both of the components that would lie at the membrane-water interface and would control ionic flux through a combination of electrostatic discrimination and size complementarity with transported guests. The latter might be amenable to control through a series of different bipyridyl components of different lengths. The appeal of such a strategy is the simplicity of the synthesis: relatively simple molecular components would spontaneously produce complex functional structures.

An obvious weakness of the strategy is the impossibility to control the relative stoichiometry of the **enPd** and **bipy** components within a two-phase membrane/water system. Each component would partition between the aqueous phase and the bilayer membrane, and the intermediates between starting components and final product would also differentially partition. Thus strict stoichiometric control as the putative channel forms is out of the question. The additional experimental variables of overall concentrations and pH make this a very difficult problem to examine experimentally. We therefore turned to the development of a practical method to allow us to probe design questions indirectly: what is the effect of total concentration, of an excess **bipy** or of a range of pH values on the "fidelity"[15] of the desired assembly?

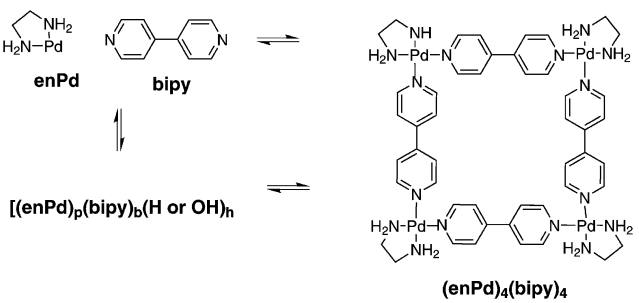

Scheme 1 Component equilibria leading to the formation of a metallosupramolecular square.

Department of Chemistry, University of Victoria, Victoria, Canada. E-mail: tmf@uvic.ca; Fax: 1 250 72 7147; Tel: 1 250 721 7150

The general thermodynamic principles have been discussed, notably by Ercolani[10,11,16,17] and by Piguet and co-workers[8,9,18–20] for binary complexes of general formula M_mL_n as found in the self-assembly of helicates (eqn (1)). Following the notation of Piguet and co-workers,[8] the cumulative formation constants for such species (β_{mn}) are given by a general form such as eqn (2):

$$m\,\mathrm{M} + n\,\mathrm{L} \rightleftharpoons [\mathrm{M}_m\mathrm{L}_n];\ \beta_{mn} \quad (1)$$

$$\beta_{mn} = \omega_{mn} \prod_{i}^{mn} k_i \prod_{i}^{mn-m-n+1} c^{\mathrm{eff}} \prod_{i<j}^{n} u_{ij}^{\mathrm{MM}} \prod_{k<l}^{m} u_{kl}^{\mathrm{LL}} \quad (2a)$$

$$\log(\beta_{mn}) = \log(\omega_{mn}) + \sum_{i}^{mn} \log(k_i) + \sum_{i}^{mn-m-n+1} \log(c^{\mathrm{eff}}) + \sum_{i<j}^{n} \log(u_{ij}^{\mathrm{MM}}) + \sum_{k<l}^{n} \log(u_{kl}^{\mathrm{LL}}) \quad (2b)$$

The essence of the approach is the additive free energy term (the k_i term) in which the assembly of $[M_mL_n]$ is viewed as a series of $m \times n$ pairwise interactions of equal energy, here given as the single stepwise microscopic association constant k_i. This first-order approach is modified by the inclusion of terms that account for attractive or repulsive energy corrections between adjacent metal centers for each of the n ligands (u^{MM}) or adjacent ligands for each of the m metals (u^{LL}). Metallosupramolecular assembly typically involves formation of macropolycyclic structures, hence the self-assembly process can be viewed as a competition between intermolecular oligomerization reactions to produce a pool of linear structures, and intramolecular cyclization reactions to produce the final assembly.[10] Each intramolecular cyclization requires an entropic correction to the intermolecular k_i, given by the effective concentration term (c^{eff}) for each unique macrocycle in the assembly.[8] Finally the ω_{mn} term of eqn (2a,b) considers the microscopic degeneracy of the species M_mL_n.

Previous workers[11,15,18,19,21] have focused on binary systems having defined $m : n$ stoichiometry. As noted above, we are concerned with the formation of self-assembled structures over a range of stoichiometric compositions. For the specific example of the assembly of the Fujita "square", the intermediate species to consider include oligomers of **enPd** and **bipy**, protonated forms of free and coordinated **bipy**, and hydroxo complexes of **enPd**. These species are defined by eqn (3) in which stoichiometric coefficients (p, b, h) give the number of **enPd**, **bipy**, and proton/hydroxide (H) in a given complex†:

$$p\,\mathbf{enPd} + b\,\mathbf{bipy} + h\,\mathrm{H} \rightleftharpoons [(\mathbf{enPd})_p(\mathbf{bipy})_p(\mathrm{H})_h];\ \beta_{pbh} \quad (3)$$

Eqn (3) represents a complete collection of species within the multi-component self-assembly process that produces the $(\mathbf{enPd})_4(\mathbf{bipy})_4$ square. The goal of this study is to develop a method that will allow the numerical estimation of the required values of β_{pbh} for such a complicated system and the use of these values to probe the stability of the self-assembly product over a concentration and pH range. We report the development of the method, new experimental data required for input values to the calculation, and the results of solution speciation simulations that provide insights into the nature of multi-component assembly.

† Charges are omitted for clarity. Hydroxide is a stoichiometric sink of protons hence hydroxo complexes are represented by species with negative values of the coefficient h.

Results and discussion

Method to estimate cumulative formation constants

Although eqn (2a,b) offers a general structure, our predictive method requires inputs that can be determined from model systems (k_i term) or from geometrical considerations (the c^{eff} and the ω_{mn} term). The u^{MM} and u^{LL} terms, although theoretically sound, are not generally amenable to *a priori* prediction or direct measurement. Since they act as a perturbation on the k_i term, our approach is to recognize a number of different types of k_i terms within the structure, and to use inputs derived from experimental model systems that are appropriate for each type. This practical expedient diminishes generality, but produces the practical outputs required.

The stoichiometric coefficients (p, b, h) of the intermediate species $[(\mathbf{enPd})_p(\mathbf{bipy})_b(\mathrm{H})_h]$ are related through the structural constraints of the system. Each **enPd** fragment can form at most two linkages (to **bipy** or hydroxide) and each **bipy** can form at most two linkages (to **enPd** or protons). Species with two or more **enPd** are linked by $p - 1$ **bipy** therefore the number of **bipy** is constrained to the range $p + 1 \geq b \geq p - 1$. For these same oligomeric species the number of terminal bipy groups available for protonation is $b - p + 1$. Similarly the number of terminal **enPd** centers available for binding hydroxide is two minus the number of terminal **bipy** hence the range of h is $b - p + 1 \geq |h| \geq 0$. A positive h indicates a protonated complex; a negative h indicates a hydroxo complex.† Considering dimeric to hexameric linear oligomers as likely species in relatively dilute solutions ($2 \leq p \leq 6$), these constraints define a set of 45 species derived from the three reactants (**enPd**, **bipy**, proton/hydroxide). A further ten monomeric species (*pbh*) are considered: two protonated **bipy** species (*pbh* = ***011***, ***012***), mono- and bis-bipy complexes of **enPd** (***110***, ***120***) and their four protonated and hydroxo complexes (***11−1***, ***111***, ***121***, ***122***), and two **enPd** hydroxo complexes (***10−2***, ***20−2***). The species **enPd**OH (***10−1***) is not included since it is known to be a minor species; the corresponding dimer $(\mathbf{enPd})_2(\mathrm{OH})_2$ (***20−2***) is the predominant species detected experimentally.[22] Finally, pK_w was included (species ***00−1***) to give a total of 56 species to be considered in the simulation. Implicit in the foregoing discussion is the assumption that the **enPd** fragments do not themselves undergo substitution or redistribution of the ethylenediamine ligands. Such processes are known to be slow, due in part to the very high thermodynamic stability of the **enPd** complex ($\log(\beta_{\mathrm{enPd}} = 23.4)$.[23]

A priori, any linear species with 1 : 1 **enPd** : **bipy** stoichiometry could be a precursor to a cyclic structure. Only cyclic species of general formula $(\mathbf{enPd})_{2n}(\mathbf{bipy})_{2n}$ ($n > 1$) will form strain-free cyclic structures that preserve the 90° N–Pd–N angle at the square planar palladium centers. There is evidence for cyclic trimers with capping ligands other than ethylene diamine or with extended **bipy** analogs, but the only structure

observed with **enPd** corners is the square tetramer.[14,24] At a given concentration, higher oligomers formed in the additive model implied by eqn (2) are progressively less favored simply by mass action. The cyclic tetramer having *pbh* stoichiometry ***440*** is therefore the most abundant strain-free cyclic structure and the sole cyclic structure considered; the case of a putative cyclic trimer is examined below.

The entropic term for the formation of cyclic species (c^{eff}) is principally related to the restriction of rotations around single bonds as a linear precursor closes to the cyclic structure.[8,25] The effective molarity for closure of a self-assembled Zn–porphyrin tetramer was estimated computationally to be greater than 0.1 M and was found experimentally to be 20 M.[16] Ring closure in this system involves seven rotors: three Zn–pyridine N bonds and four pyridine–porphyrin single bonds. This range of values is in line with the general expectation for closure of a bifunctional precursor with seven rotors (2.7 M) to a strain-free macrocycle.[25] The closure of the ***440*** species involves eleven rotors (seven Pd–pyridine N plus four bipyridyl single bonds) for which an EM of about 0.3 M would be expected.[25] This is likely to be a minor term in the overall analysis and for simplicity we assume that $c^{\mathrm{eff}} = 1$ ($\log(c^{\mathrm{eff}}) = 0$). The overall effect of this assumption is reviewed below.

The microscopic degeneracy factor of eqn (2), defined by the equilibrium of eqn (3), is given by eqn (4):[9,11,26]

$$\omega_{pbh} = \frac{\sigma_{\mathrm{enPd}}^{p}\sigma_{\mathrm{bipy}}^{b}\sigma_{\mathrm{H}}^{h}}{\sigma_{(\mathrm{enPd})_p(\mathrm{bipy})_b(\mathrm{H})_h}^{pbh}} \qquad (4)$$

The symmetry numbers of **enPd, bipy**, and proton/hydroxide (σ_{enPd}, σ_{bipy}, σ_{H}) are 2, 2, and 1, respectively reflecting the two equivalent binding sites on **enPd** and **bipy** and the unique binding site on a proton or hydroxide ligand. Square-planar geometry about each Pd^{2+} and free rotation about each Pd–pyridine bond ensures that all possible species are achiral and conformationally averaged. As a direct consequence, the species $(\mathbf{enPd})_p(\mathbf{bipy})_b(\mathrm{H})_h$ with $h = \pm 1$, or with $p = b$ has $\sigma = 1$, otherwise the value is 2. The cyclic species ***440*** has fourfold symmetry, hence $\sigma = 4$.

The square-planar geometry about each Pd^{2+} center and the linear extension afforded by each **bipy** also ensures that ligand–ligand and metal–metal interactions are minimized. Even so the binding of a second **bipy** to a given Pd^{2+} center will differ from the first binding. Similarly, the intermetallic interaction, such as occurs in the binding of a second **enPd** to a given **bipy,** will also differ from the first **enPd**–**bipy** interaction. As opposed to regarding this as a perturbation of a unitary interaction (k_i as modified by the u^{MM} and u^{MM} terms of eqn (2a,b)),[8,9] we enumerate these separate interactions explicitly. The species are viewed as composed of a sum of the five microscopic step-wise equilibria given in Scheme 2: a 1 : 1 **enPd**–**bipy** interaction given by k_1, binding of a second **bipy** to an **enPd**–**bipy** center given by k_2, binding of a second **enPd** to an **enPd**–**bipy** center given by k_b, protonation of a terminal **enPd**–**bipy** (k_{H}) and hydrolysis of a terminal **enPd** center (k_{OH}).

With these component equilibria defined, the cumulative formation constants of the oligomeric linear species *pbh* are given by eqn (5a) for protonated species ($p \geq 2$; $h \geq 0$) and by eqn (5b) for hydroxo complexes ($p \geq 2$; $h \leq 0$). We view

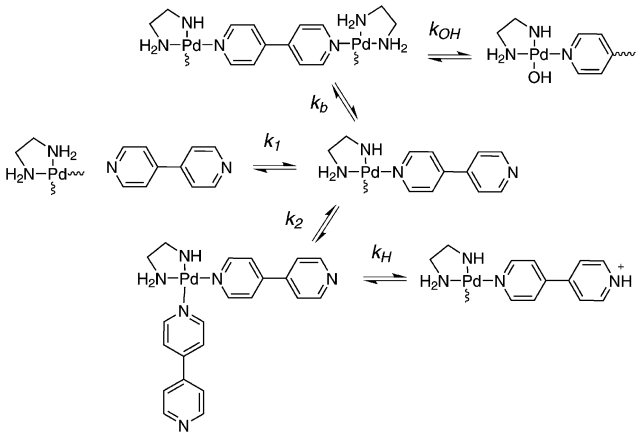

Scheme 2 Microscopic stepwise equilibria required to generate $(\mathbf{enPd})_p(\mathbf{bipy})_b(\mathrm{H})_h$ species.

the species as assembled from an initial **bipy**–**enPd** interaction (k_1), followed by the $(p - 2)$ k_2 interactions to initiate the **bipy** bridges and the $(p - 1)$ k_b interactions to terminate the **bipy** bridges in the oligomers. To this skeleton are added $(b - p + 1)$ terminal **bipy** as k_2 interactions to give a total of $(b - 1)$ k_2 interactions. Hydroxo or protonated contributions (if required) are then added to the skeleton as required by the stoichiometric coefficient h. A similar additive approach can be used to generate the $\log(\beta_{pbh})$ values for the monomeric species where these are not directly available from experiment.

$$\log(\beta_{pbh}) = \log(\omega_{pbh}) + \log(k_1) + (b - 1)\log(k_2) + (p - 1)\log(k_b) + h\log(k_{\mathrm{H}}) \qquad (5a)$$

$$\log(\beta_{pbh}) = \log(\omega_{pbh}) + \log(k_1) + (b - 1)\log(k_2) + (p - 1)\log(k_b) + |h|\log(k_{\mathrm{OH}}) \qquad (5b)$$

Eqn (5a,b) apply to linear oligomers. Cyclic oligomers ($p = b$) must include a c^{eff} entropic correction term (even though it is small as discussed above) and must involve an additional bridging **bipy** interaction to close the cycle. Thus the $\log(\beta_{pb0})$ values for such species are given by eqn (6). As discussed above, we initially focus only on $p = b = 4$, but eqn (6) is general.

$$\log(\beta_{pb0}) = \log(\omega_{pb0}) + \log(k_1) + (b - 1)\log(k_2) + p\log(k_b) + \log(c^{\mathrm{eff}})\ \{\text{where } p = b\} \qquad (6)$$

Experimental values for input to the calculation

The stepwise constants for the component equilibria defined in Scheme 2 are not directly available from experiment, thus we examined systems which would provide reasonable models of each one. As shown in Scheme 3, we chose 3-phenylpyridine (**3-PhPy**) as a model for the interactions around a single palladium center based on the close similarity of the basicities of **bipy** and **3-Phpy**,[27] and the diethylenetriamine complex of palladium (**dienPd**) with **bipy** to probe the bridging interactions between palladium centers. A closer structural and electronic analog might have been an *N*-pyridylmethyl-

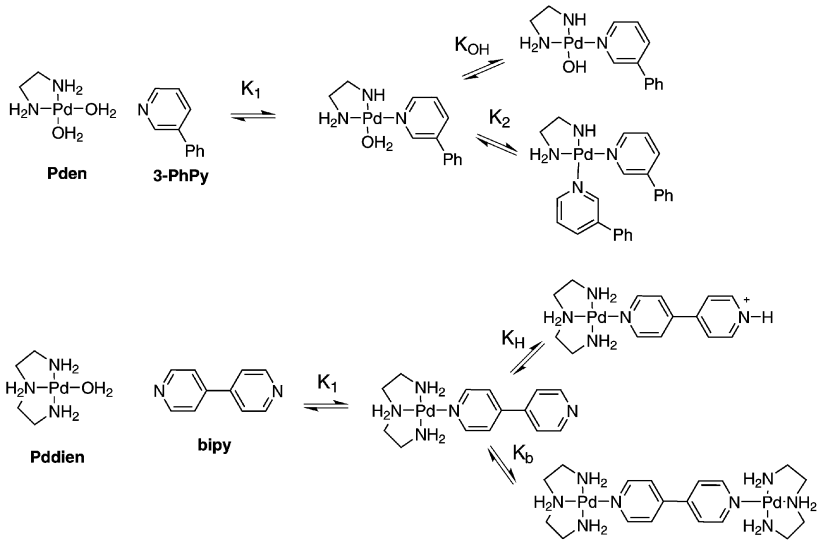

Scheme 3 Macroscopic stepwise equilibria of model compounds.

ethylenediamine complex[28] but the compound proved to have very complicated hydroxo speciation chemistry that complicated the subsequent analysis.

There is a limited amount of literature data for these systems, so the required values were determined by potentiometric titration.[30,31] Each component (**enPd**, **dienPd**, **3-PhPy**, **bipy**; 1–5 mM in 0.1 M KNO_3 plus HNO_3 in slight excess) was titrated with NaOH and the resultant pH-volume data were treated with Hyperquad[32] to yield protonation and hydrolysis constants. The titrations were repeated for various **enPd** : **3-PhPy** and **dienPd** : **bipy** ratios and pH–volume data were again processed with Hyperquad[32] to produce a set of cumulative formation constants from which the required stepwise constants can be derived as defined in Scheme 3. For example: in the **enPd** : **3-PhPy** series the experimental value of $\log(\beta_{110})$ is $\log(K_1)$, $\log(\beta_{120}) = \log(\beta_{110}) + \log(K_2)$, and $\log(\beta_{11-1}) = \log(\beta_{110}) + \log(K_{OH})$. Similarly, in the **dienPd** : **bipy** series $\log(\beta_{110})$ is $\log(K_1)$, $\log(\beta_{210}) = \log(\beta_{110}) + \log(K_b)$, and $\log(\beta_{111}) = \log(\beta_{110}) + \log(K_H)$. The required microscopic constants can then be derived through consideration of the microscopic degeneracy for each of the stepwise equilibria calculated using eqn (4). The experimental values of $\log(\beta_{pbh})$ and derived values of $\log(k_i)$ are given in Table 1.

Where literature values are available, the agreement is acceptable. The largest deviations are in the hydroxo complexes of **enPd**. Our titration data fit adequately to a simple model involving only monomeric dihydroxo and bridged dihydroxo species; more complex hydroxo speciation has been reported,[22] but this might simply reflect differences in the ionic media (nitrate *vs*. perchlorate). For single component systems, the experimental precision as assessed from replicates is ±0.1 in $\log(\beta)$. In multi-component systems the precision is ±0.2 in $\log(\beta)$, thus the propagation of errors gives a precision of ±0.2 in $\log(k_1)$ and ±0.4 in the other $\log(k_i)$ values. Where alternative estimates of the derived values occur they fall within the experimental precision. The effect of the experimental uncertainties on the outputs of the simulations and conclusions is examined below.

Calculated speciation

The experimental estimates of the values of $\log(k_i)$ and eqn (4)–(6) were used to generate a set of $\log(\beta_{pbh})$ values for the 51 (of 56) species that cannot be directly determined experimentally. Experimental $\log(\beta_{pbh})$ values for **enPd** hydroxo species and protonated **bipy** species and the literature value for pK_w completed a set of values needed as inputs for the calculation (see Experimental section for values). The speciation was calculated from assumed reactant concentrations and pH ranges using the program HySS.[33] Typical output is given in Fig. 1 for two **enPd** concentrations and a range of **enPd : bipy** stoichiometries. The low **enPd** concentration of 10 μM was selected to illustrate a number of minor species in competition with the desired ***440*** species; the 5 mM concentration is typical of published spectra and binding studies.[12,13]

The species indicated in Fig. 1 are the ones that reach a significant fraction (>10%) of the total **enPd** at some pH between 3 and 9. Even though some mixtures are reasonably complicated, the majority of the species remain as minor components with the result that the overall speciation is consistent with relatively simple interpretations. For example with **enPd** in excess, species containing two **enPd** units are well represented (Fig. 1(A): ***210***, ***21−1***, ***20−2***, ***21−2***) and are collectively more important than the ***440*** complex. Conversely in excess **bipy** species with a 1 : 2 **enPd : bipy** stoichiometry are well represented (Fig. 1(C): ***122***, ***121***, ***120***). The ***440*** complex is certainly the dominant species at a 1 : 1 **enPd : bipy** stoichiometry, and is predominant over a wide pH range at the higher concentration (Fig. 1(D)). Even in this case however, a collection of minor hydroxo complexes place a limit of about pH 8 as the basic end of the range of the ***440*** stability.

The overall speciation is more usefully displayed as given in Fig. 2 as a "map" in pH–[**bipy**] "space" for two concentrations **enPd**. The third dimension of these contour plots is the vertical axis of Fig. 1 *i.e*. the percentage of the total **enPd** held in the indicated complex.

Table 1 Experimental values of cumulative formation constants log(β_{pbh}) and derived values of microscopic constants[a]

Pd species (p)	Pyridyl species (b)	Complex stoichiometry (pbh)	log(β_{pbh})	Lit. value[ref]	log(ω_{pbh})	Derived step (k_i)	log(k_i)
enPd	—	***10–1***	—[b]	−6.68[22]			
		10–2	−14.7	−14.52[23]			
		20–2	−8.1	−7.76[23]			
dienPd	—	***10–1***	−7.1	−7.2[29]	0	k_{OH}	−6.9
—	**bipy**	***011***	4.71	4.77[27]			
		012	7.48	7.46[27]			
—	**3-Phpy**	***011***	4.70	4.81[27]			
enPd	**3-Phpy**	***110***	5.9		−0.3	K_1	6.2
		120	11.2		0	k_2	5.2
		11–1	−0.8		−0.3	k_{OH}	−6.5
dienPd	**bipy**	***110***	6.0		−0.3	k_1	6.3
		210	11.2		0	k_b	5.2
		111	10.2		−0.3	k_H	4.5
—	—	***00–1***	—	−13.77[27]			

[a] Determined by potentiometric titration (I = 0.1 M KNO_3; 25 °C). [b] A complex of this stoichiometry was not needed for an acceptable fit.

As with Fig. 1, the species indicated in Fig. 2 are the only ones that account for greater than 10% of the total **enPd** at any point; the display is truncated at 40% for clarity of presentation. At both concentrations the extent of formation of the square complex ***440*** is constrained by competing species. At 10 μM the system is finely balanced between competing protonated species (lower part of Fig. 2—left), competing monomeric species (left side), competing hydroxo species (upper edge) and competing bis-**bipy** complexes (right side). The combination provides a "region of abundance" for the ***440*** complex between pH 4 and 7 and a 0.4–4 **enPd : bipy** ratio. At the higher concentration of 5 mM (Fig. 2—right), the same competition is evident, but additional bridging **bipy** species emerge (***212***, ***21–2***) as a result of a more favorable mass action

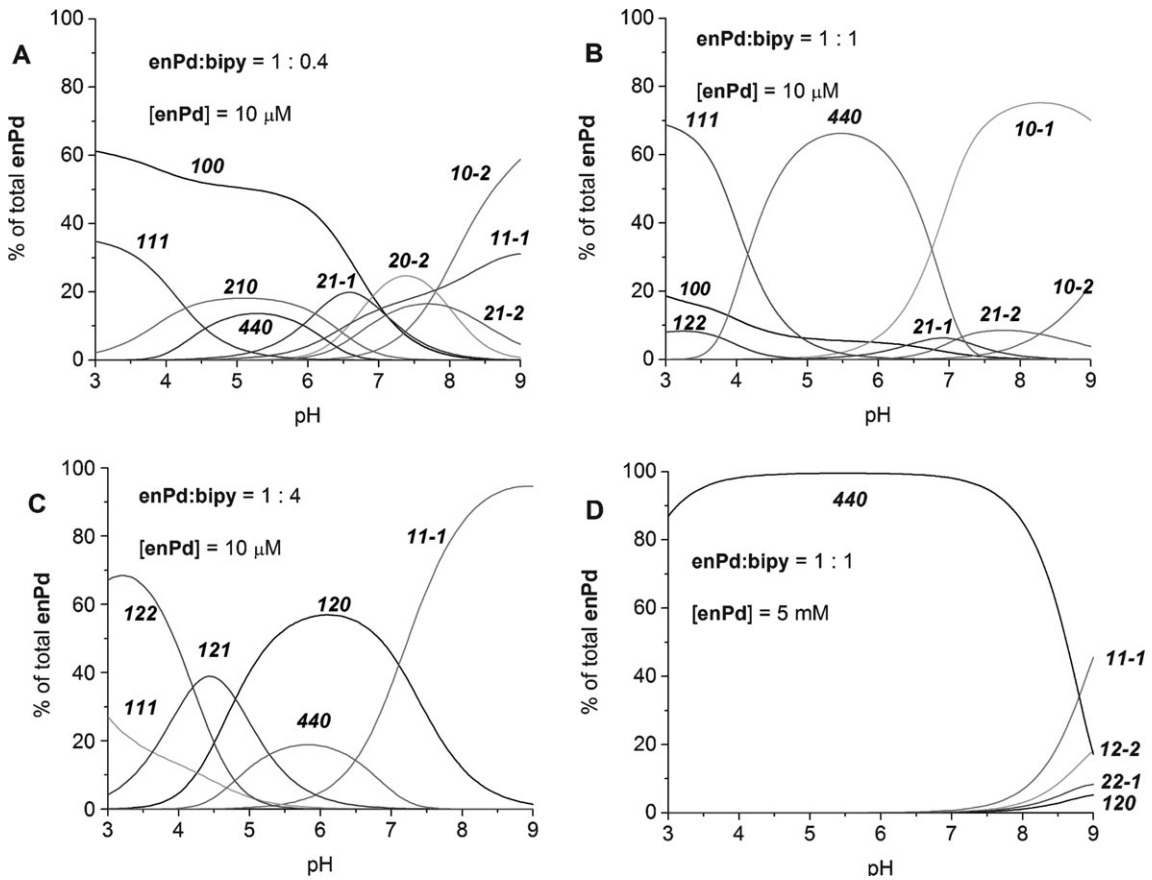

Fig. 1 Speciation of **enPd** : **bipy** mixtures.

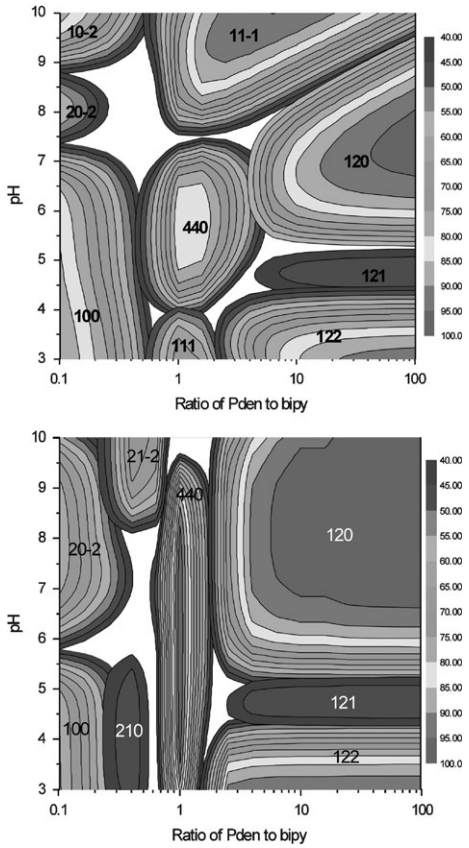

Fig. 2 Speciation maps for **enPd–bipy** mixtures at 10 μM (top) and 5 mM (bottom) total **enPd** concentration.

term relative to the pH. The net result is that the ''window of abundance'' of the ***440*** complex is significantly narrowed in the **bipy** dimension even as it is elongated in the pH dimension. Stated another way, increasing the **enPd** concentration expands the range of pH stability but tightly restricts the **enPd : bipy** range over which the ***440*** complex forms.

How well does the model reproduce the available experimental data? The original report of the formation of the square ***440*** complex also reported an NMR titration in which the **enPd : bipy** ratio was progressively altered from 1 : 0.2, to 1 : 0.4, 1 : 0.6, and finally 1 : 0.9.[13] The NMR spectral changes were interpreted as three species in slow exchange: the bridged dimer ***210***, a linear trimer ***320***, and the cyclic ***440***. The spectral overlap makes quantitative comparison difficult, but qualitatively the spectra show ***210*** significantly more abundant than ***320*** at 1 : 0.2, ***210*** about equal to ***440*** and somewhat more abundant than ***320*** at 1 : 0.4, ***440*** more abundant than ***210*** or ***320*** at 1 : 0.6 and virtually exclusive formation of ***440*** at 1 : 0.9. These results are in excellent qualitative agreement with the calculated speciation as shown in Fig. 3. The experimental pH is not reported, but could be assumed to be pH 4–5 as a result of carbon dioxide from the air or trace mineral acid. In this pH range the relative abundances and the changes as the concentration is varied are directly comparable between the calculation and the reported spectra and the overall agreement with experimental data is remarkably good.

As noted above, we omitted the cyclic trimer complex ***330*** on the basis that it would be subject to strain. The available experimental data show no evidence for such a species,[2] which we interpret as the abundance of a ***330*** species to be less than 10% of the abundance of ***440***. The $\log(\beta_{330})$ of the linear trimer is 28.9. A hypothetical strain-free cyclic ***330*** species would have an additional $\log(k_b)$ interaction so would have $\log(\beta_{330})_{cyc} = 34.1$. With this value included in the calculation, the cyclic ***330*** complex completely swamps any contribution from ***440*** under all stoichiometric conditions. Trial and error variation in the value of $\log(\beta_{330})_{cyc}$ suggests that this parameter could take a maximum value of about 31.6 before it would contribute greater than 10% of the total **enPd** in competition with ***440*** and the other species in Fig. 3. The ''triangle-square'' equilibrium in 4,4′-bipyridylacetylene is concentration dependent running from 8% triangle at 80 mM to 18% triangle at 8 mM;[34] a value of $\log(\beta_{330})_{cyc}$ of about 32 is required to reproduce these ratios (80 mM, 10%; 8 mM, 17%). The ''destabilization'' of the cyclic species by 2–2.5 log units relative to the hypothetical strain-free cyclic species corresponds to an energetic difference of the order of 12–15 kJ mol^{-1}. This can be interpreted as the strain energy required to deform the three Pd corners from 90° in order to close the macrocycle. This might be included in eqn (6) as an unfavorable $\log(c^{eff})$ term or be included in an extended equation as an additional explicit term for angle deformation $\log(u_\theta)$. Either way this term would be about −2 to −2.5 log units for the ***330*** species.

The method is based on an additive free energy approach in which the individual contributing terms were derived from experiment hence are subject to experimental error. As noted above this factor amounts to ±0.4 in the $\log(k_i)$ values. What influence does this factor have on the outputs as illustrated in Fig. 1–3? This question was explored through the comparison of the outputs of different simulations derived from different values of $\log(k_i)$. Cases where all interactions are weaker by $\log(k_i) = -0.4$ or stronger by $\log(k_i) = 0.4$ give very closely similar outputs at 10 μM. This is not surprising since the species are in competitive equilibria and the component interaction energies are fairly comparable, so the overall system undergoes relatively little differentiation. The acidity and hydrolysis contributions (k_H, k_{OH}) similarly have relatively little effect when allowed to increase or decrease by ±0.4 log units relative to fixed contributions from the Pd–pyridyl interactions. These terms generally act to contract or expand the pH range of the protonated/hydroxo species with concomitant expansion/contraction in the ranges of the non-protonated/hydroxo species ranges. The changes are small relative to the wide range of pH values possible. Every derived value of $\log(\beta_{pbh})$ contains a single contribution from $\log(k_1)$ (eqn (5) and (6)) and the values of $\log(\beta_{pbh})$ are uniformly large with respect to ±0.4 log units. As a consequence, uncertainty in this parameter makes very little difference in the overall output from of the calculation.

Conversely, the individual contributions of $\log(k_2)$ and $\log(k_b)$ are replicated $(b - 1)$ and $(p - 1)$ times, respectively. Experimentally these terms were found to be the same; hence we could anticipate a ''worst case'' in which one of the terms was underestimated and the other overestimated. The case with $\log(k_2) = 5.2 + 0.4 = 5.6$ and $\log(k_b) = 5.2 - 0.4 = 4.8$ was explored as an example of this type of ''worst case''. The

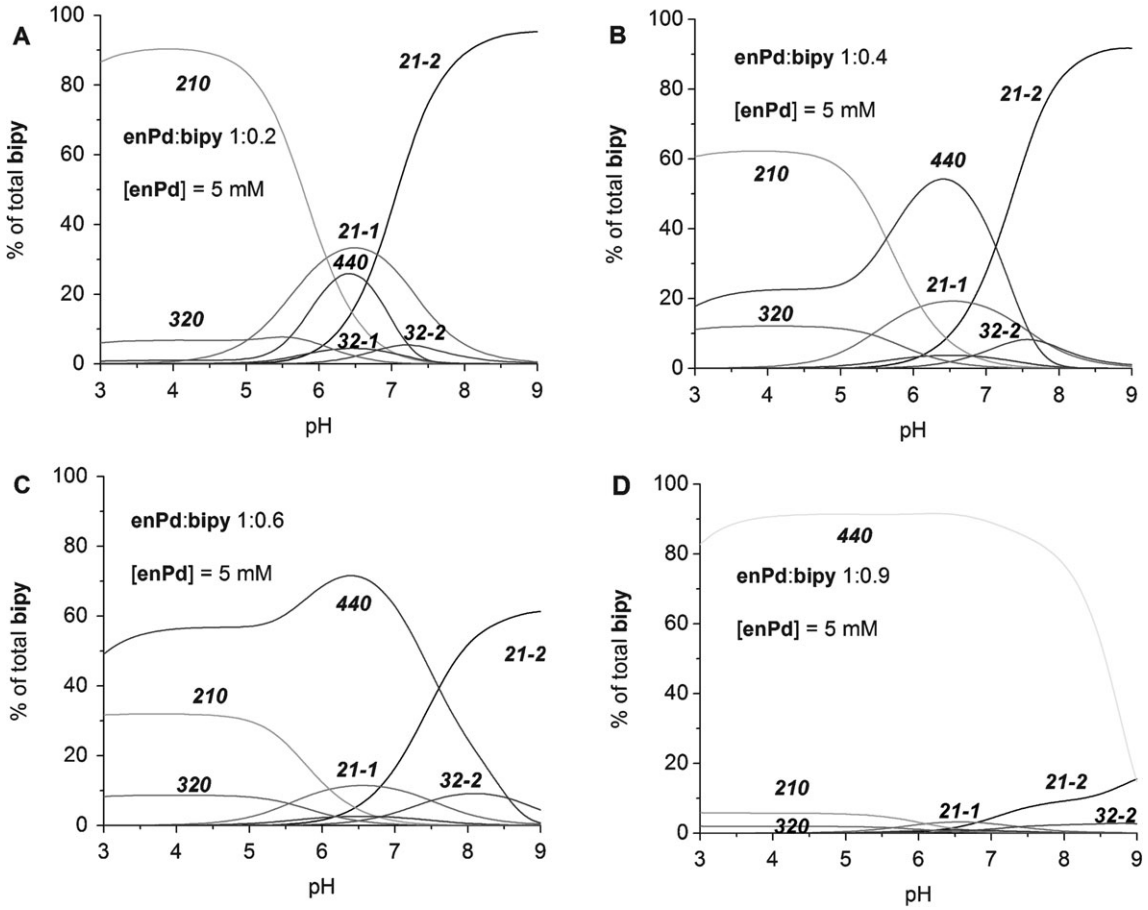

Fig. 3 Speciation of **enPd**–**bipy** mixtures calculated for the conditions of NMR experiments previously reported.[13]

results are illustrated in Fig. 4 in which an example from each of Fig. 1 and 3 are given. In the case of Fig. 4(A) in comparison to Fig. 1(A) there are minor differences in the balance between the ***210*** and ***440*** species but the remainder of the diagram is very similar. The Fig. 4(B) to Fig. 3(C) comparison is very close, and either version would support the discussion of the NMR spectra as outlined above. We therefore conclude that the outputs are relatively insensitive to the uncertainties in the values of $\log(k_i)$.

Implications

The additive free energy approach implicit in the method appears to reproduce the details of the speciation, so it is appropriate to consider the energetic implications embedded in the calculated concentrations. The "maps" of Fig. 2 show that speciation is strongly controlled by reactant concentrations. This is not surprising since the individual $\log(k_i)$ values correspond to interaction energies only of the order of $-\Delta G = 30$ kJ mol^{-1} at 298 K. The $\log(\beta_{pbh})$ values are large, but it is not the absolute magnitude that is important. Rather it is the relative magnitudes of competing processes of a given stoichiometry that need to be considered.

The formation of the ***440*** species can be seen as the product of a number of parallel bimolecular pathways in which smaller oligomeric species combine to produce a linear oligomer having the $(\mathbf{enPd})_4(\mathbf{bipy})_4$ stoichiometry that subsequently undergoes unimolecular cyclization. The linear oligomer can form by six unique bimolecular reactions as given in Table 2. Each of these processes can be written as a step-wise equilibrium in which the apparent equilibrium constant (K_{step}) is given by $\log(\beta_{lin440}) - (\log(\beta_{pbh}) + \log(\beta_{p'b'h'})$, where $\log(\beta_{lin440})$ is calculated from eqn (5). From these stepwise equilibria, the stepwise free energy change (ΔG_{step}) can be calculated as given in Table 2.

The linear ***440*** species lies 28.5 kJ mol^{-1} above the cyclic ***440*** species, thus the overall free energy change for the two-step process of bimolecular reaction to form linear ***440*** followed by intramolecular cyclization ranges from -50.0 kJ mol^{-1} for the ***220*** + ***220*** $\rightleftharpoons$ ***440*** reaction to -59.4 kJ mol^{-1} for the isomeric reaction ***100*** + ***430*** $\rightleftharpoons$ ***440*** reaction. The calculated free energy changes for this stoichiometric condition differ by less than 10 kJ mol^{-1} between the six possible pathways. From this result we conclude that the potential surface has a well-defined minimum for the ***440*** (linear and cyclized) species but is otherwise relatively flat.

Ligand substitution at Pd^{2+} generally occurs *via* an associative mechanism;[35] in all cases except ***010*** + ***430*** the incoming nucleophiles are terminal coordinated **bipy** groups that associate with a palladium center bound to **en** and a bridging **bipy**. It is reasonable to suppose that the geometric and solvation changes required in these isomeric reactions are comparable to one another. These reactions are exergonic,

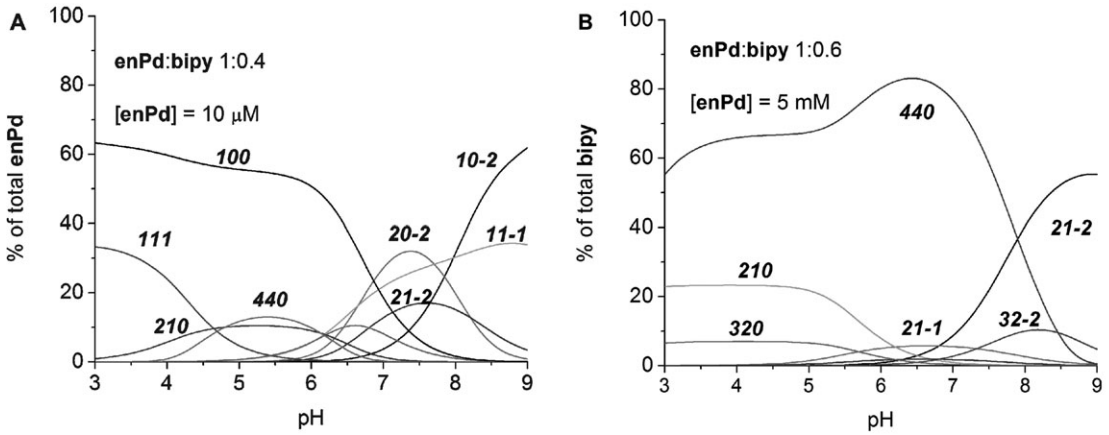

Fig. 4 Speciation calculated for **enPd**–**bipy** mixtures using a "worst case" assumption of the values of $\log(k_i)$.

hence the transition states are reactant-like. By the extra-thermodynamic assumption of the Hammond postulate, if the overall free energy changes of a set of comparable reactions are of comparable magnitude, then the transition states of the various reactions must also be energetically comparable. We therefore infer that the free energy of activation for the forward reaction leading to linear ***440*** is about the same energy above the reactants in each of the identified reactions in Table 2. It follows that the rate constants for the isomeric forward reactions are all approximately the same, since the geometrical, solvation, and energetic components of the reactions are closely similar. This does not apply to the ***010*** + ***430*** reaction, which involves a qualitatively different nucleophile.

The rate of a bimolecular reaction depends on the rate constant and the product of the reactant concentrations. The calculation gives the equilibrium concentrations of the reactant species for any set of input concentrations, thus we can compute the concentration component of the forward rate for each of the isomeric reactions leading to ***440***. Assuming the rate constants are similar, this allows an estimate of the relative rates of the parallel pathways that lead to ***440***. These values are also given in Table 2. This analysis suggests that there are kinetically preferred pathways for the formation of the ***440*** species. Intuitively, bimolecular pathways involving relatively abundant species, such as the dimerization of the ***220*** species would be expected to be faster than pathways in which one of the components is at very low concentration (*e.g.* ***340***). The analysis above is in line with this intuition.

Conclusions

It is true that these are complex solutions involving many species. In that respect they are similar to other complex systems of current interest such as dynamic combinatorial libraries. In this area as well, recourse to numerical methods to explore the behavior of the complex system has yielded useful insights.[36,37] Our approach to understanding the complexity of self-assembly numerically is based on a limited number of pair-wise interactions. The direct result is a method that produces satisfactory outputs that relate directly to experimental observations. Extensions of this approach to other systems should be straight-forward, and the method we illustrate here should provide a useful tool for the design of functional self-assembled systems. Our own application of the use of the square complex as a portal to an ion channel is reported separately.[38]

Table 2 Bimolecular processes leading to linear $(\mathbf{enPd})_4(\mathbf{bipy})_4$

Reactants *pbh* + *p′b′h′*	$\log(K_{step})$	$-\Delta G_{step}$/kJ mol^{-1}	k_{rel}
010 + ***430***	5.4	30.9	—
100 + ***340***	5.4	30.9	1
210 + ***230***	4.4	25.0	10
120 + ***320***	4.4	25.0	13
110 + ***330***	3.8	21.5	40
220 + ***220***	3.8	21.5	50

Experimental

All reagents were obtained from commercial sources and were used without further purification unless noted otherwise. Stock solutions were prepared using boiled and cooled water in volumetric glassware. NaOH was standardized using potassium hydrogen phthalate which was then used to standardize the HNO_3 solution. Standardized 0.2 M HNO_3 was added using a microlitre syringe to protonate all the basic sites in the 4,4′-bipyridine (**bipy**) and 3-phenylpyridine stock solutions. (Ethylenediamine)palladium(II) dinitrate ($\mathbf{enPd}(NO_3)_2$) was prepared and characterized according to a published procedure:[39] $\mathbf{enPd}Cl_2$ (0.1487 g, 0.6277 mmol) was suspended in ~2 ml water, 2.50 ml of 0.4991 M $AgNO_3$ was added, the resultant slurry was stirred for 4 h then vacuum filtered to recover a lemon yellow solution which was transferred quantitatively through a 0.45 μm syringe filter and diluted to 25.0 ml with water. Diethylenetriamine palladium(II) dibromide was prepared and characterized according to a published procedure[40–42] (^{1}H NMR (D_2O): δ 2.46–3.09 (m) ppm. MS (FAB) m/z: 207.9 [53%], 245 [100%]). To prepare the $Pd(dien)(ClO_4)_2$ stock solution, $Pd(dien)Br_2$ (0.2570 g, 0.5837 mmol) was dissolved in ~2 ml water, $AgClO_4$ (0.2631 g, 1.167 mmol dissolved in ~1 ml water) was added with stirring, the resultant was stirred for 6 h at 40 °C then vacuum filtered to recover a light yellow solution which was transferred quantitatively through a 0.45 μm syringe filter and diluted to 25.0 ml

with water. $Pd(dien)(ClO_4)_2$ could not be made from the chloride derivative because the metathesis with $AgClO_4$ was not complete.

The titrations were carried out using a Mettler DL21 automatic titrimeter as recently described[30] in a closed jacketed glass cell kept at 25 ± 0.2 °C under a nitrogen atmosphere. The electrode circuit was set up as follows: Ag/AgCl|4 M KCl|0.1 M KNO_3. The electrodes were calibrated daily from a strong acid–strong base titration protocol.[30] Sample solutions were prepared from stock solutions in 10 ml volumetric flasks. In order to ensure that all basic sites were protonated, 100 μl of standardized 0.2 M acid was added to the solutions. Solutions with at least three different **enPd** to 3-phenylpyridine (or **dienPd** to **bipy**) molar ratios were prepared and titrated for each model system. Each titration was usually carried out in duplicate with at least 52 points per titration curve. The titration curves were fitted using the program HyperQuad.[32]

Speciation was calculated using the program HySS.[33] Values used in the calculation (*pbh*, $\log(\beta_{pbh})$): ***00−1***, −13.77; ***10−2***, −14.7; ***20−2***, −8.4; ***011***, 4.7; ***012***, 7.5; ***110***, 6.8; ***120***, 12.1; ***11−1***, 0.4; ***111***, 11.3; ***122***, 21.1; ***121***, 16.9; ***21−2***, −0.9; ***21−1***, 5.9; ***210***, 12; ***22−1***, 11.4; ***220***, 17.9; ***221***, 22.4; ***230***, 23.1; ***231***, 27.9; ***232***, 32.1; ***32−2***, 10.1; ***32−1***, 16.9; ***320***, 23.1; ***33−1***, 22.4; ***330***, 28.9; ***331***, 33.4; ***340***, 34.1; ***341***, 38.9; ***342***, 43.1; ***43−2***, 21.1; ***43−1***, 27.9; ***430***, 34.1; ***44−1***, 33.4; ***440***, 44.5; ***441***, 44.4; ***450***, 45.1; ***451***, 49.9; ***452***, 54.1; ***54−2***, 32.2; ***54−1***, 38.9; ***540***, 45.1; ***55−1***, 44.5; ***550***, 50.9; ***551***, 55.4; ***560***, 56.2; ***561***, 61; ***562***, 65.2; ***65−2***, 43.2; ***65−1***, 50; ***650***, 56.4; ***66−1***, 55.5; ***660***, 61.7; ***661***, 66.5; ***670***, 67.2; ***671***, 72; ***672***, 76.2.

Acknowledgements

The support of the Natural Sciences and Engineering Research Council of Canada is gratefully acknowledged.

References

1 J. A. Thomas, in *Encyclopedia of Supramolecular Chemistry*, ed. J. L. Atwood, Marcel Dekker, New York, 2004, pp. 1248–1256.
2 M. Fujita, M. Tominaga, A. Hori and B. Therrien, *Acc. Chem. Res.*, 2005, **38**, 369–378.
3 S. R. Seidel and P. J. Stang, *Acc. Chem. Res.*, 2002, **35**, 972–983.
4 M. Yoshizawa and M. Fujita, *Science*, 2006, **312**, 251–254.
5 M. Yoshizawa and M. Fujita, *Pure Appl. Chem.*, 2005, **77**, 1107–1112.
6 M. Schmittel and V. Kalsani, *Top. Curr. Chem.*, 2005, **245**, 1–53.
7 J. Rebek, Jr, *Angew. Chem., Int. Ed.*, 2005, **44**, 2068–2078.
8 J. Hamaczek, M. Borkovec and C. Piguet, *Dalton Trans.*, 2006, 1473–1490.
9 C. Piguet, M. Borkovec, J. Hamacek and K. Zeckert, *Coord. Chem. Rev.*, 2005, **249**, 705–726.
10 G. Ercolani, *J. Phys. Chem. B*, 2003, **107**, 5052–5057.
11 G. Ercolani, *J. Am. Chem. Soc.*, 2003, **125**, 16097–16103.
12 M. Fujita, S. Nagao, M. Iida, M. Ogata and K. Ogura, *J. Am. Chem. Soc.*, 1993, **115**, 1574–1576.
13 M. Fujita, J. Yazaki and K. Ogura, *J. Am. Chem. Soc.*, 1990, **12**, 5645–5647.
14 M. Fujita, in *Comprehensive Supramolecular Chemistry*, ed. J.-P. Sauvage and M. W. Hosseini, Elsevier Science, Amsterdam/New York, 1996, vol. 9, pp. 253–282.
15 E. M. Todd, J. R. Quinn, T. Park and S. C. Zimmerman, *Isr. J. Chem.*, 2005, **45**, 381–389.
16 G. Ercolani, M. Ioele and D. Monti, *New J. Chem.*, 2001, **25**, 783–789.
17 G. Ercolani, *J. Phys. Chem. B*, 1998, **102**, 5699–5703.
18 J. Hamaczek, M. Borkovec and C. Piguet, *Chem. Eur. J.*, 2005, **11**, 5227–5237.
19 J. Hamaczek, M. Borkovec and C. Piguet, *Chem. Eur. J.*, 2005, **11**, 5217–5226.
20 M. Borkovec, J. Hamaczek and C. Piguet, *Dalton Trans.*, 2004, 4096–4105.
21 J. Hamaczek and C. Piguet, *J. Phys. Chem. B*, 2006, **110**, 7783–7792.
22 J. M. Tercero-Moreno, A. Matila-Hernadez, S. Gonzalez-Garcia and J. Niclos-Gutierrez, *Inorg. Chim. Acta*, 1996, **253**, 23–29.
23 G. Andregg, *Inorg. Chim. Acta*, 1986, **111**, 25–30.
24 M. Fujita, M. Aoyagi and K. Ogura, *Inorg. Chim. Acta*, 1996, **246**, 53–57.
25 C. Galli and L. Mandolini, *Eur. J. Org. Chem.*, 2000, 3117–3125.
26 J. T. Edsall and J. Wyman, *Biophysical Chemistry: Thermodynamics, Electrostatics, and the Biological Significance of the Properties of Matter*, Academic Press, New York, 1958.
27 A. E. Martell and R. M. Smith, *Critical Stability Constants*, Plenum Press, New York, 1976.
28 A. Hofmann, D. Jaganyi, O. Q. Munro, G. Liehr and R. van Eldik, *Inorg. Chem.*, 2003, **42**, 1688–1700.
29 Z. Bugarcic, B. Petrovic and R. Jelic, *Transition Met. Chem.*, 2001, **26**, 668–671.
30 L. I. Bosch, T. M. Fyles and T. D. James, *Tetrahedron*, 2004, **60**, 11175–11190.
31 A. E. Martell and R. J. Motekaitis, *Determination and Use of Stability Constants*, VCH Publishers, New York, 1992.
32 A. Sabatini, A. Vacca and P. Gans, *Talanta*, 1996, **43**, 53–65.
33 L. Alderighi, P. Gans, A. Ienco, D. Peters, A. Sabatini and A. Vacca, *Coord. Chem. Rev.*, 1999, **184**, 311–318.
34 M. Fujita and K. Ogura, *Coord. Chem. Rev.*, 1996, **148**, 249–264.
35 D. T. Richens, *Chem. Rev.*, 2005, **105**, 1961–2002.
36 P. T. Corbett, S. Otto and J. K. M. Sanders, *Chem. Eur. J.*, 2004, **10**, 3139–3143.
37 K. Severin, *Chem. Eur. J.*, 2004, **10**, 2565–2580.
38 T. M. Fyles and C. C. Tong, *New J. Chem.*, 2007, **31**, DOI: 10.1039/b610660a.
39 R. Ahlrichs, M. Ballauff, K. Eichkorn, O. Hanemann, G. Kettenbach and P. Klufers, *Chem. Eur. J.*, 1998, **4**, 835–844.
40 F. Basolo, W. H. Baddley and K. J. Weidenbaum, *J. Am. Chem. Soc.*, 1966, **88**, 1576–1581.
41 P.-K. F. Chin and F. R. Hartley, *Inorg. Chem.*, 1976, **15**, 982–984.
42 F. L. Wimmer, S. Wimmer, P. Castan and R. J. Puddephatt, *Inorg. Synth.*, 1992, **29**, 185–187.

